*Sensors and Materials*, Vol. 18, No. 5 (2006) 277–282
MYU Tokyo

S & M 0649

# Preparation of Ultrafine $ZnFe_2O_4$ and Its Gas-Sensing Properties for $Cl_2$

Jianzhou Zhang*, Donghui Chen and Liang Chen

School of Environmental Science and Engineering, Donghua University, 2999 Renmin Rd. North,
Songjiang District, Shanghai, 201620, China

***Key words*****:** $Cl_2$ sensor, $ZnFe_2O_4$, microemulsion, semiconductor, spinel-type oxide

Ultrafine $ZnFe_2O_4$, a $Cl_2$ gas-sensing material has been successfully fabricated by a novel polyoxyethylene lauryl ether + n-hexanol/n-heptance/water (zinc nitrate + ferrum nitrate) W/O microemulsion method. The composition and structure of the powder have been detected by X-ray diffraction analysis (XRD) and transmission electron microscopy (TEM). The results show that the as-made $ZnFe_2O_4$ has a spinel-type structure, and the size of each spherical particle is 30 nm with good dispersiveness. The effect of temperature on the sensitivity of sensors, gas sensor's selectivity, the effect of gas concentration, and response and recovery characteristics are investigated at the optimum working temperature of 270°C. The measurement of gas-sensing properties of the $ZnFe_2O_4$ sensors indicates that these sensors have high sensitivity, excellent selectivity and quick-response behavior to $Cl_2$ gas. The gas-sensing mechanism is also discussed.

## 1. Introduction

Chlorine gas is very useful in many fields, such as a raw material in chemical industries, a bleaching reagent, and a disinfectant of water. Chlorine gas, however, is harmful to humans because of its strong oxidizing power. To protect humans and the natural environment from chlorine damage, sensing devices with high sensitivity and reliability are required in many fields. The detection of $Cl_2$ using electrochemical(1,2) and metal-phthalocyanine sensors(3,4) has been reported. On the other hand, there are few studies on semiconductor-type chlorine gas sensors. Spinel-type semiconducting $ZnFe_2O_4$ has been studied focusing on gas-sensing properties for $NO_X$,(5) $H_2S$(6) and $C_2H_5OH$.(7) However, studies on its sensitivity to $Cl_2$ gas have rarely been reported. In this study, we prepared ultrafine $ZnFe_2O_4$ by a novel microemulsion method and analyzed its gas-sensing properties for $Cl_2$. In this paper, the sensing mechanism is discussed.

---

*Corresponding author, e-mail address: zhangjianzhou@mail.dhu.edu.cn

## 2. Experimental Methods

### 2.1 *Preparation of $ZnFe_2O_4$*

All reagents were purer than 99.9% and used without further purification. Polyoxyethylene lauryl ether, n-hexanol and n-heptance were mixed together at a certain weight ratio. $Zn(NO_3)\cdot_26H_2O$ and $Fe(NO_3)_3\cdot 9H_2O$ (molar ratio = 1:2) were dissolved in distilled water. The latter mixture was slowly dropped in the former mixture at 25°C until a transparent W/O microemulsion system formed. When ammonia solution was slowly dropped, a chemcal reaction occurred. The mixture was constantly stirred for 1 h to ensure that the interactants were mixed thoroughly and had reacted completely. After centrifuging and washing using distilled water and alcohol-acetone solutions alternately, $Zn(OH)_2$ and $Fe(OH)_3$ were obtained. The coprecipitate was dried at 80°C for 24 h, then calcined at 800°C for 3 h. After grinding using an agate pestle and mortar, ultrafine $ZnFe_2O_4$ powder was obtained.

### 2.2 *Analysis of $ZnFe_2O_4$*

The structure and crystal state of the product were obtained using an X-ray diffractometer (Germany Bluker D8-Advance ) with Cu K$\alpha$ radiation (wavelength $\lambda = 1.5406$ Å) operating at 20 mA and 40 kV. Data were collected by a step-scanning method for $10° \leq 2\theta \leq 70°$, with a step width of 0.05° and a step time of 1 s. The size and shape of the particles were analyzed by transmission electron microscopy (Japan JEM-100SX).

### 2.3 *Measurements of gas-sensing properties*

The $ZnFe_2O_4$ powder was deposited between interdigital gold electrodes on the outer wall of ceramic tubes using terpilenol. Electrical contacts were prepared with 0.05 mm platinum wires attached to the gold electrodes. Then, the deposited powder was annealed at 600°C for 1 h. After aging for 10 days, the obtained sensors were set up in a glass test chamber with a volume of 0.18 $m^3$ and kept under a continuous flow of fresh air for 30 min before measurement. Operating voltage ($V_H$) was supplied to either of the coils for heating the sensors, and circuit voltage ($V_C = 10$ V) was supplied across the sensors and the load resistor ($R_L = 1$ M$\Omega$) connected in series. The signal voltage across the load, which changed with the type and concentration of gas, was measured. The gas sensitivity to $Cl_2$, $NO_2$, $C_2H_5OH$, $H_2S$ and acetone was measured. A given amount of each gas was injected into the chamber and mixed with air by a fan for 30 s. Sensitivity to gases, $S$, is defined as the ratio of the resistance of the sensor in the test gas to that in dry air. If the resistance in the test gas is increases, the sensitivity of the sensor is defined as $S = R_{gas}/R_{air}$, and the sensor is of the p-type. Otherwise, it is defined as $S = R_{air}/R_{gas}$, and the sensor is of the n-type,(8) where $R_{gas}$ and $R_{air}$ are the resistances of the sensor in test gas and dry air, respectively.

## 3. Results and Discussion

### 3.1 *Composition and structure of $ZnFe_2O_4$*

Figure 1 shows the X-ray diffraction pattern of as-made $ZnFe_2O_4$ powder. XRD measurements revealed that the peaks of the spin-type complex oxide are all assigned to the franklinite phase of $ZnFe_2O_4$ (JCPDS 22-1012). According to the Scherrer formula, the size of a $ZnFe_2O_4$ particle is about 37 nm. The TEM image (Fig. 2) shows that $ZnFe_2O_4$

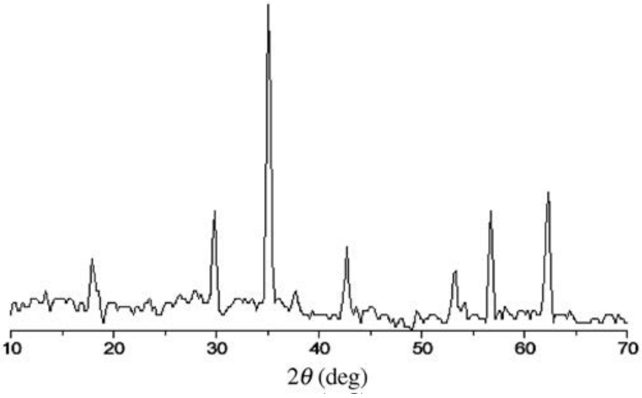

Fig. 1. XRD pattern of $ZnFe_2O_4$.

Fig. 2. TEM of $ZnFe_2O_4$ powder.

consists of spherical particles with a uniform grain size distribution. The average grain size is about 30 nm, which is consistent with that obtained from the Scherrer formula.

### 3.2 *Gas-sensing properties of $ZnFe_2O_4$ sensors*

In general, operating temperature affects the sensitivity of sensors. The higher the temperature, the more the surface reaction of the sensor is enhanced and the higher the sensitivity within a temperature range. Figure 3 shows the relationship between gas sensitivity and operating temperature at 50 ppm $Cl_2$; ppm refers to the volume concentration of $Cl_2$ in the gaseous mixture. The results indicate that the gas sensitivity of the sensor increases with operating temperature up to the optimum operating temperature of 270°C. Further increasing the operating temperature reduces the sensitivity. The $ZnFe_2O_4$ sensor's selectivity was also tested, as shown in Fig. 4. Except for $Cl_2$, $C_2H_5OH$, $H_2S$, acetone and $NO_2$ were all tested at a concentration of 50 ppm at 270°C. These experimental results indicate that $ZnFe_2O_4$ sensor is insensitive to these gases, compared with its sensitivity to

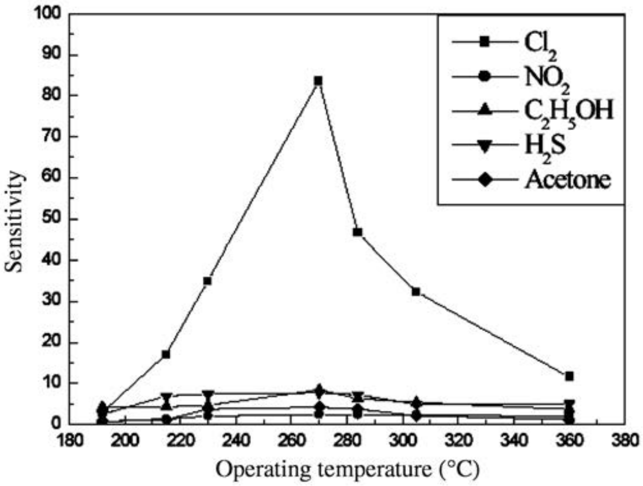

Fig. 3. Gas sensitivity to all tested gases as function of operating temperature.

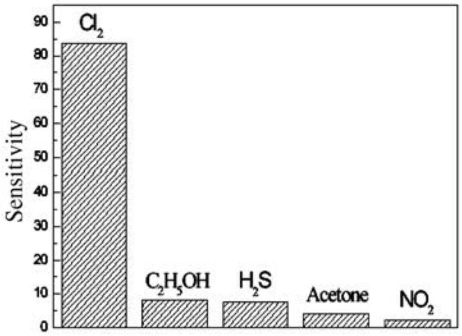

Fig. 4. Sensitivity of $ZnFe_2O_4$ sensor to all tested gases

$Cl_2$ gas. The sensitivity to $Cl_2$ gas is about 8 times higher than that to other tested gases. Furthermore, we found that the gas sensitivity of the sensor increases with increasing $Cl_2$ concentration, as shown in Fig. 5. Therefore, the $ZnFe_2O_4$ sensor exhibits both high sensitivity and excellent selectivity to $Cl_2$ gas. Figure 6 shows the response-recovery characteristic of $ZnFe_2O_4$ sensor. After the introduction of 50 ppm $Cl_2$, the response appears immediately. The 90% response time and the 90% recovery time are 4 and 30 s, respectively.

### 3.3 *Sensing mechanism*

The decrease in the conductivity of n-type semiconducting $ZnFe_2O_4$ following the introduction of $Cl_2$ gas is attributed to the following mechanism: chlorine molecules are adsorbed on the $ZnFe_2O_4$ surface as negatively charged ions, trapping electrons from $ZnFe_2O_4$. Generally, oxygen molecules are adsorbed on the $ZnFe_2O_4$ surface in air,

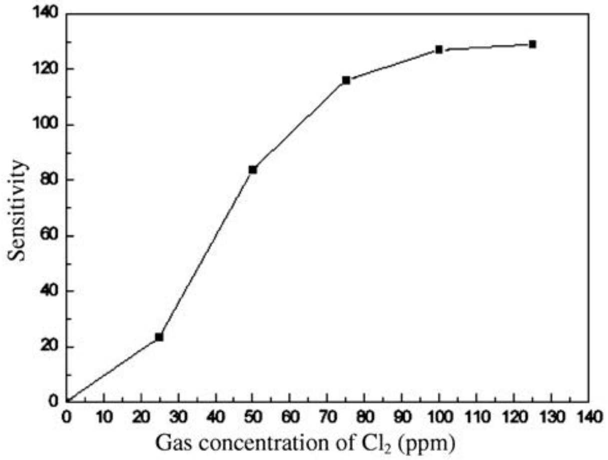

Fig. 5. Sensitivity of $ZnFe_2O_4$ sensor vs concentration of $Cl_2$.

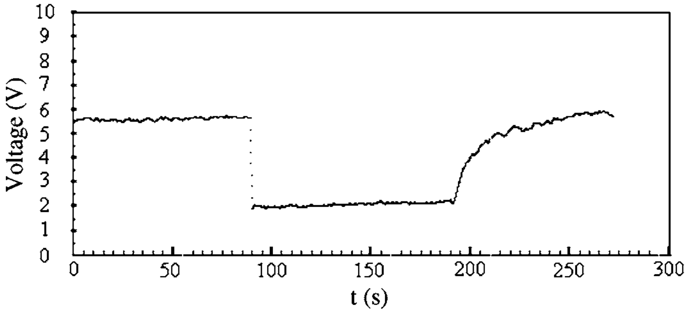

Fig. 6. Response-recovery characteristic of $ZnFe_2O_4$ sensor to 50 ppm $Cl_2$ at 270°C.

trapping electrons. When introducing $Cl_2$ gas, chlorine molecules adsorbed on the $ZnFe_2O_4$ surface should also trap electrons owing to the strong electronegativity of the chlorine atom. Thus, chlorine and oxygen are competitively adsorbed on the $ZnFe_2O_4$ surface. With the increase in temperature, the adsorbed oxygen molecules begin to desorb from the $ZnFe_2O_4$ surface, and chlorine molecules are adsorbed dissociatively, as shown in the following equation.

$$1/2Cl_2(g) + e^- \longleftrightarrow Cl^-(ads)$$

The electron comes from $ZnFe_2O_4$, which is consumed in the reaction, reducing the extent of the decrease in the conductivity of $ZnFe_2O_4$. Because the sensing mechanism is related to adsorption, the condition of the surface is, therefore, an important factor. Particles with a small grain size and a regular surface are good for enhancing sensitivity. Thus, the novel W/O microemulsion preparation method is effective.

## 4. Conclusions

$ZnFe_2O_4$ is an important gas-sensing material. We developed a novel W/O microemulsion technique for the preparation of $ZnFe_2O_4$ and analyzed its gas-sensing properties for $Cl_2$. On the basis of the results presented in this paper, the following conclusions can be drawn:

(1) N-type semiconducting $ZnFe_2O_4$ can be prepared using a novel W/O microemulsion: Polyoxyethylene lauryl ether + n-hexanol/n-heptance/water (zinc nitrate + ferrum nitrate).

(2) The XRD results show that the product is spinel-type $ZnFe_2O_4$. The TEM image shows that $ZnFe_2O_4$ particles are spherical with a uniform grain size distribution and an average grain size of 30 nm.

(3) The gas-sensing properties of the $ZnFe_2O_4$ sensor indicates that these sensors exhibit high sensitivity, excellent selectivity and quick-response behavior to $Cl_2$ gas.

## References

1 C. M. Mari, G. Terzaghi, M. Bertolini and G. B. Barbi: Sens. Actuators, B **8** (1992) 41.
2 H. Aono, E. Sugimoto, Y. Mori and Y. Okajima: Chem. Lett. **6** (1993) 1039.
3 C. Nylander: J. Phys. E: Sci. Instrum. **18** (1985) 736.
4 T. Miyata, S. Kawaguchi, M. Ishii and T. Minami: Thin Solid Films **425** (2003) 255.
5 N. Miura, S. Zhuiykov and N. Yamazoe: Sens. Actuators, B **83** (2002) 222.
6 N. Xinshu, L.Yanli and X. Jiaqiang: J. Funct. Mater. **34** (2002) 413.
7 C. Xiangfeng, L. Xingqin and Guangyao: Sens. Actuators, B **55** (1999) 19.
8 L. Hongming, T. Shah-jye, H. Peng-jan and T. Wenli: Nano. Mater. **10** (1998) 465.